

Reliability-based topology optimization using a new method for sensitivity approximation - application to ground structures

Ke Liu¹ · Glaucio H. Paulino¹ · Paolo Gardoni²

Received: 19 August 2015 / Revised: 30 November 2015 / Accepted: 10 January 2016 / Published online: 2 April 2016
© Springer-Verlag Berlin Heidelberg 2016

Abstract This paper proposes an efficient gradient-based optimization approach for reliability-based topology optimization of structures under uncertainties. Our objective is to find the optimized topology of structures with minimum weight which also satisfy certain reliability requirements. In the literature, those problems are primarily performed with approaches that use a first-order reliability method (FORM) to estimate the gradient of the probability of failure. However, these approaches may lead to deficient or even invalid results because the gradient of probabilistic constraints, calculated by first order approximation, might not be sufficiently accurate. To overcome this issue, a newly developed segmental multi-point linearization (SML) method is employed in the optimization approach for a more accurate estimation of the gradient of failure probability. Meanwhile, this implementation also improves the approximation of the probability evaluation at no extra cost. In general, adoption of the SML method leads to a more accurate and robust approach. Numerical examples show that the new approach, based on the SML method, is numerically

stable and usually provides optimized structures that have more of the desired features than conventional FORM-based approaches. The present approach typically does not lead to a fully stressed design, and thus this feature will be verified by numerical examples.

Keywords Topology optimization · Reliability analysis · Sensitivity analysis · Reliability-based topology optimization

1 Introduction

Topology optimization helps engineers design structures that provide most efficient use of material with desired structural behavior. In recent years, topology optimization has been applied to engineering problems in a wide range of fields, for example, building design, vehicle design, material design, and medical treatment (e.g., craniofacial reconstruction) (Rozvany 2001; Bendsøe and Sigmund 2003; Sutradhar et al. 2010). Most research has been formulated in a deterministic manner, however, deterministic topology optimization may have limited use for realistic design problems where the inherent uncertainties in loading conditions, material properties and manufacturing process cannot be neglected. There are two main strategies to address this concern, namely robust topology optimization, and reliability-based topology optimization (RBTO) (Schüeller and Jensen 2008). The goal of the robust topology optimization is to find a structure that is relatively insensitive with respect to uncertainties in design conditions or manufacturing process (Schevenels et al. 2011; Zhao and Wang 2014). On the other hand, the RBTO aims to account for the effect of uncertainties on structural performance in terms of failure probability during the topology optimization process. The advantage

✉ Glaucio H. Paulino
paulino@gatech.edu

Ke Liu
kliu89@gatech.edu

Paolo Gardoni
gardoni@illinois.edu

¹ School of Civil and Environmental Engineering, Georgia Institute of Technology, Atlanta, GA 30332, USA

² Department of Civil and Environmental Engineering, University of Illinois, Urbana, IL 61801, USA

of the RBTO formulation is that it allows a quantitative management of the uncertainties.

Topology optimization can be carried out in many different ways, for example, the density approach, the ground structure approach, the level-set approach, etc (Bendsøe and Sigmund 2003). The density approach as well as the level-set approach aims to find the best material distribution within a continuum (Bendsøe and Sigmund 2003; Talisch et al. 2012). In this paper, the ground structure approach is adopted because it provides directly the truss layout on a base grid so that it is particularly suitable for design of modular space structures (Topping 1992; Beghini et al. 2014), which is common for designs of building or bridge structures. A typical ground structure approach extracts the optimal structural layout from a very dense set of potential joints and bars by sizing the members and allowing them to vanish (Achtziger et al. 1992; Ben-Tal and Bendsøe 1993; Sokół T 2011; Zegard and Paulino 2014).

As a design problem, the RBTO can be regarded as a subtopic of the reliability-based design optimization (RBDO), which has a rich literature. The RBDO performs design optimization in conjunction with reliability analysis by defining probabilistic constraints due to the presence of random variables. The RBDO is typically performed at two levels (Nguyen et al. 2010, 2011): component reliability-based design optimization, which considers each failure mode individually, and system reliability-based design optimization, which deals with a combination of failure modes simultaneously. A generic formulation for component RBDO considering one reliability component can be given as follows:

$$\begin{aligned} \min_{\mathbf{x}} \quad & f(\mathbf{x}) \\ \text{s.t.} \quad & P_f = \int_{G(\mathbf{x}, \mathbf{u}) < 0} \varphi_n(\mathbf{u}) d\mathbf{u} \leq P_f^t \\ & h_k(\mathbf{x}) \leq 0; \quad k = 1, 2, 3, \dots \end{aligned}$$

where \mathbf{x} is the vector of design variables to be selected in the optimization process; \mathbf{u} is the vector of random variables that are transformed from the original distribution space to standard normal space by a probability preserving transformation (Choi et al. 2006); $f(\mathbf{x})$ is the objective function; $G(\mathbf{x}, \mathbf{u})$ is the limit state function for structural behavior such that for a given design \mathbf{x} , a realization of \mathbf{u} that makes $G < 0$ is considered a failure event; $\varphi_n(\cdot)$ is the n -variate standard normal probability density function (PDF); P_f^t is the threshold on failure probability; and h_k 's are deterministic constraints such as lower and upper bounds of design variables. The probabilistic constraint can also be stated in terms of reliability or reliability index. The reliability is defined as the complement of the probability of failure as $R = 1 - P_f$, and the corresponding reliability index is $\beta = \Phi^{-1}(R)$ (Ditlevsen and Madsen 1996), where $\Phi(\cdot)$

is the cumulative distribution function (CDF) of a standard normal distribution.

The RBDO problems can be solved using either gradient-free (Mathakari et al. 2007) or gradient-based methods. In this work, we will mainly focus on gradient-based methods. There are two major gradient-based approaches for RBDO (Tu et al. 2001): the Reliability Index Approach (RIA), which directly solves the probability constrained optimization problem using the sensitivities of the probabilistic constraints; and the Performance Measure Approach (PMA), which constructs target performance function(s) by an inverse reliability analysis and solves a deterministic optimization problem for each iteration. The two approaches are usually implemented in conjunction with a first-order reliability method (FORM), which is an approximation method for reliability analysis (Ditlevsen and Madsen 1996). Therefore, if FORM or inverse FORM is used in RIA or PMA respectively, it is known that they are mathematically equivalent if the probabilistic constraint is active (Tu et al. 2001), although PMA tends to be more robust than RIA. In other words, the commonly used RIA and PMA approximate the failure probability P_f and its gradient with respect to design variables $\nabla_{\mathbf{x}} P_f$ at the same level of accuracy, indicating that the optimized solutions by both methods satisfy the same approximation of the Karush-Kuhn-Tucker (KKT) optimality conditions. There are also some variations of these two approaches, for example, Royset et al. (2001a, b, 2006) proposed decoupled RBDO formulations that use a more thorough inverse reliability analysis than the traditional FORM-based PMA and allows for heuristic updates of probability approximation by other reliability analysis methods, for example second order reliability method (SORM) and Monte Carlo simulation (MCS).

Direct implementation of RIA or PMA results in a double loop optimization scheme since the reliability analysis or inverse reliability analysis requires an iterative process to find the most likely failure point or the most probable point (MPP) (Tu et al. 2001). In order to reduce the computational cost, single loop algorithms (Cheng et al. 2006; Liang et al. 2007; McDonald and Mahadevan 2008; Nguyen et al. 2010) have been developed, which simplifies the inner loop of the optimization, and use explicit estimations instead of full reliability analysis or inverse reliability analysis. Some researchers have implemented these methods to solve RBTO problems. Nguyen et al. (2011) applied a single loop algorithm to system RBTO performed on a density based multi-resolution topology optimization. Mogami et al. (Mogami et al. 2006) employed a traditional double loop RIA to solve RBTO problems on ground structures. Other methods such as Monte Carlo simulation based stochastic optimization (Royset and Polak 2004) and equivalent

perturbation based robust optimization (Jalalpour et al. 2011) are also used to perform RBTO.

However, FORM only takes a first order approximation of the limit state surface, and both the values of the probability of failure and its sensitivity are estimated by collecting information from a single point on the limit state surface (Rackwitz 2001). Therefore, FORM-based approximations are insufficient to capture a limit state function that is non-linear with respect to both random variables and design variables. In particular, the errors in the estimated sensitivities can become quite significant, which is explained with more details in Section 3. In reliability-based optimization problem, the importance of the accuracy of sensitivity information can be observed by examining the optimality conditions of the optimization problem. The KKT conditions for a general component RBDO problem as described before are given by:

- (1) Stationarity condition: $\nabla_{\mathbf{x}}f + \lambda \nabla_{\mathbf{x}}P_f + \sum \gamma_i \nabla_{\mathbf{x}}h_i = 0$
- (2) Primal feasibility: $P_f - P_f^t \leq 0, h_k \leq 0 \forall k$
- (3) Dual feasibility: $\lambda \geq 0, \gamma_k \geq 0 \forall k$
- (4) Complementary slackness: $\lambda(P_f - P_f^t) = 0, \gamma_k h_k = 0 \forall k$

For most gradient-based numerical algorithms, the solution that satisfies the KKT conditions is the optimized one that they are looking for. Therefore, if approximations of the terms have to be adopted, they are always preferred to be as accurate as possible. In general, the more accurate we can estimate P_f and $\nabla_{\mathbf{x}}P_f$, the closer the solution is to a local optimum. FORM-based RBDO methods typically use a first-order approximation of the limit state function both to estimate the probability of failure and its sensitivity with respect to design variables. Some studies (Nguyen et al. 2011; Royset et al. 2006) proposed hybrid FORM-based RBDO approaches where SORM, MCS or other reliability methods are used to improve the estimations of the failure probability, but they still compute the sensitivity based on a first-order approximation of the limit state function. Although the primal feasibility condition is approximated with a better accuracy, little attention has been paid to the accuracy of the approximations involved in the stationarity condition (i.e., the approximations of the sensitivities), which may actually be more influential to the solution of RBDO. Particularly, because the number of design variables is typically very large in RBTO, the final topology can be severely affected by the errors in the sensitivity estimation. In addition, the errors can progressively accumulate during the iterative process of the optimization because the sensitivity determines the search direction at each iteration step. Thus, the accuracy of the estimation of sensitivity is critical. For RBTO, the need for an accurate estimation of

the sensitivity of the probabilistic function has not been clearly addressed, and a first-order approximation of the sensitivity, which is typically not sufficiently accurate, is widely used.

Thus this research adopts a new method named segmental multi-point linearization (SML) (Liu 2014; Liu et al. 2015) in conjunction with RIA to solve RBTO problems. The SML method provides generally more accurate estimations of the sensitivity of the probability of failure with respect to design variables than the commonly adopted FORM-based approximation by piece-wise linearly approximating the limit state surface using multiple segments of hyperplanes. While less essential, the SML method also improves the accuracy of the estimations of the failure probability obtained in the reliability analyses involved in the optimization. The RBTO problem concerned in this paper is truss layout optimization restraining probability of excessive compliance. The structure being optimized is discrete (lattice-based), however, the design space as well as the random space is continuous.

The remaining of the paper is structured as follows: Section 2 describes the sensitivity analysis of the probabilistic functions and the effect of the error in their approximation. Section 3 puts forward the novel segmental multi-point linearization and Section 4 addresses the formulation of RBTO considered in this paper. Section 5 provides numerical examples of RBTO in 2D and 3D. Finally conclusions are provided in Section 6.

2 Sensitivity analysis of probability functions

In order to employ gradient-based algorithms, sensitivity analysis is essential. Deterministic formulation of topology optimization has been studied extensively and the gradients of the objective function and deterministic constraints have been derived. However, challenge arises due to the presence of a probabilistic objective function or constraint(s). In this section, for completeness of the paper, we derive the analytical expression for the gradient of the probability of failure with respect to the optimization design variables. The design variables in this paper are assumed to be the parameters that defines the limit state function(s). Different derivations and thorough analyses of the parameter sensitivities of probabilistic functions can be found in the references (Breitung 1991; Uryasev 1994).

Consider a general expression for a probabilistic constraint as $P(G(\mathbf{u}, \mathbf{x}) < 0) \leq P_f^t$, and assume that the limit state function $G(\mathbf{u}, \mathbf{x})$ is continuous and differentiable. The gradient of the failure probability, with respect to the design variables, can be interpreted as the change of P_f due to a perturbation in \mathbf{x} , the design variables. Considering a pertur-

bation δx_i on one of the design variables, the corresponding change in the failure probability is given as:

$$\delta P_f = \int_{\Omega'} \varphi_n(\mathbf{u}) d\mathbf{u} - \int_{\Omega} \varphi_n(\mathbf{u}) d\mathbf{u} = \int_{\delta\Omega} \varphi_n(\mathbf{u}) d\mathbf{u} \quad (1)$$

where $\Omega = \{\mathbf{u} | G(\mathbf{u}, \mathbf{x}) < 0\}$ and $\Omega' = \{\mathbf{u} | G(\mathbf{u}, \mathbf{x} + \delta x_i \mathbf{e}_i) < 0\}$ are the failure domain of the limit state function $G(\mathbf{u}, \mathbf{x})$ before and after the perturbation δx_i is imposed. The difference between Ω and Ω' is denoted as $\delta\Omega$. The vector \mathbf{e}_i is a vector of zeros except for its i -th component that equals 1. When all the components of \mathbf{x} are fixed, except x_i , we can define a new function G^e that is equivalent to the perturbed limit state function $G(\mathbf{u}, x_i, \hat{\mathbf{x}})$:

$$G^e(\mathbf{u}, x_i) = G(\mathbf{u}, x_i, \hat{\mathbf{x}}) \quad (2)$$

where $\hat{\mathbf{x}}$ are the fixed design variables which includes all except the i th variable in \mathbf{x} . In the augmented total space of \mathbf{u} and x_i , the limit state surface in the random space can be regarded as a level set of the implicit function $G^e(\mathbf{u}, x_i) = 0$ as shown in Fig. 1. The Hamilton-Jacobi equation describes the transformation of the limit state surface due to change in x_i :

$$\nabla_{\mathbf{u}} G^e \delta \mathbf{u} + \frac{\partial G^e}{\partial x_i} \delta x_i = 0 \quad (3)$$

The term $\delta \mathbf{u}$ can be interpreted as a field of infinitesimal movement of the limit state surface in the random space, which is defined on the entire limit state surface as indicated

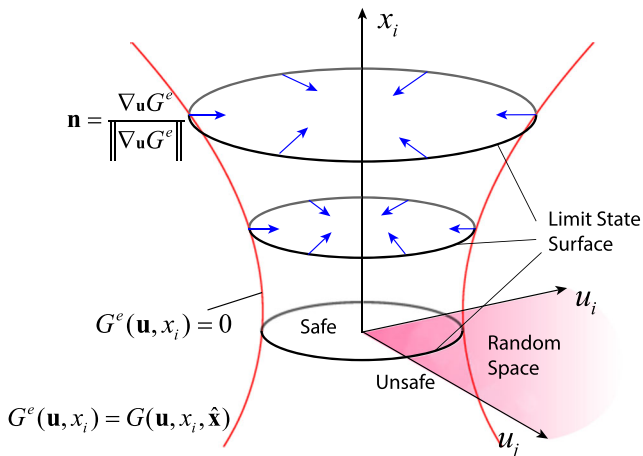


Fig. 1 Graphical illustration of the relationship between limit state surface and the level set function $G^e(\mathbf{u}, x_i) = 0$. The shaded area indicates the first quadrant of the random space

by the arrows in Fig. 1. The change of failure domain then can be expressed as:

$$\delta\Omega = \int_S \delta \mathbf{u}^T \mathbf{n} dS \quad (4)$$

where S represents the limit state surface before δx_i is imposed and \mathbf{n} is the normal direction of the limit state surface, which is positive when pointing toward the safe domain. Because $\mathbf{n} = \nabla_{\mathbf{u}} G^e / \|\nabla_{\mathbf{u}} G^e\|$, then (4) can be rewritten as:

$$\delta\Omega = \int_S \frac{\delta \mathbf{u}^T \nabla_{\mathbf{u}} G^e}{\|\nabla_{\mathbf{u}} G^e\|} dS \quad (5)$$

Substituting (3) and (5) into (1), we can obtain:

$$\delta P_f = \int_S -\frac{\varphi_n(\mathbf{u})}{\|\nabla_{\mathbf{u}} G^e\|} \frac{\partial G^e}{\partial x_i} \delta x_i dS \quad (6)$$

Rearranging terms of (6) and taking the limit of $\delta x_i \rightarrow 0$, we can obtain the derivative of P_f with respect to x_i as:

$$\frac{\partial P_f}{\partial x_i} = \lim_{\delta x_i \rightarrow 0} \frac{\delta P_f}{\delta x_i} = - \int_S \frac{\varphi_n(\mathbf{u})}{\|\nabla_{\mathbf{u}} G\|} \frac{\partial G^e}{\partial x_i} dS \quad (7)$$

Since (7) applies to each component of \mathbf{x} , the gradient of P_f with respect to \mathbf{x} becomes a surface integral on the limit state surface:

$$\nabla_{\mathbf{x}} P_f = - \int_S \frac{\varphi_n(\mathbf{u})}{\|\nabla_{\mathbf{u}} G\|} \nabla_{\mathbf{x}} G dS \quad (8)$$

For most cases, the integral in (8) cannot be computed exactly because it is a multi-dimensional surface integral. The compromise is to use approximations instead of exact evaluations. Actually, in RBDO, the probability of failure itself is often approximated.

3 Segmental multi-point linearization for approximating sensitivity

A commonly used approach to approximate the sensitivity of a probability is derived in consistence with FORM. In many reliability analysis methods including FORM, the original space of the random variables is often transformed into a standard normal space. The FORM then takes a first order expansion of the transformed limit state surface at the point that has the largest probability density, i.e., the most likely failure point, which is also called the design point. The hyperplane defined by the first order expansion is used as an approximation of the limit state surface. The resulting estimation of the sensitivity, which is adopted in most FORM-based algorithms for optimization, was derived by

Hohenbichler and Rackwitz (1986), and has the following form:

$$\nabla_{\mathbf{x}} P_f = -\frac{\varphi(\beta)}{\|\nabla_{\mathbf{u}} G^*\|} \nabla_{\mathbf{x}} G^* \tag{9}$$

where

$$\mathbf{u}^* = \min_{\mathbf{u}} \{\|\mathbf{u}\| \mid G(\mathbf{u}) = 0\} \tag{10}$$

Equation (10) is the definition of design point. The design point \mathbf{u}^* is a point on the limit state surface that is closest to the origin of the standard normal space (Ditlevsen and Madsen 1996; Rackwitz 2001). Intuitively, it is the point that represents a limit state event that is most likely to happen. The term G^* denotes $G(\mathbf{x}, \mathbf{u}^*)$, which is the limit state function evaluated at the design point. Equation (9) is equivalent as taking the integration of (8) on the hyperplane defined by the first order expansion at the most likely failure point. In some cases, the FORM-based approximation of the sensitivity may not properly reflect the change of limit state surface with respect to changes in the design variables. For example, if the design update has an impact only on the curvature of the limit state surface, the obtained sensitivity which is based on a linear approximation of the limit state surface, would not capture this change at all, as shown in Fig. 2. Whereas the approximation of failure probability by FORM might remain relatively accurate as the change only happens in low probability density region. Essentially, the FORM-based approximation of sensitivity is a differentiation of the FORM computed failure probability, and such operation usually enlarges the error. Examples and detailed comparisons can be found in reference (Liu et al. 2015). Although the impact of the errors in sensitivity estimations may differ for different RBTO problems, our numerical examples

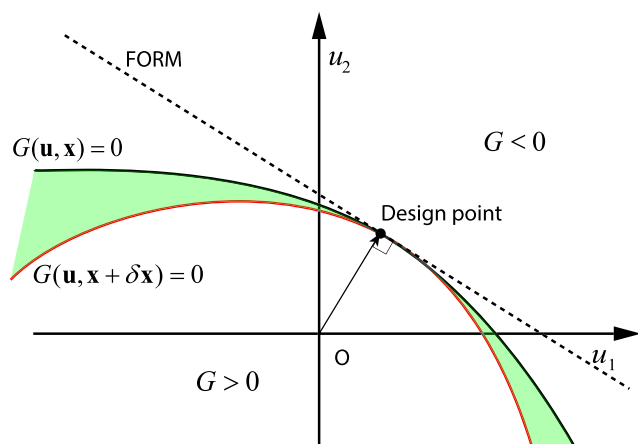


Fig. 2 A scenario when the FORM-based estimation fails to reflect the true sensitivity. The limit state surface after and before a design update ($\delta\mathbf{x}$) have the same design point. A FORM-based approximation observes that the design update does not change the limit state surface, thus the sensitivity is zero, which is not true

will show that the error in sensitivity estimation can have a significant impact on the obtained optimized topology, and FORM-based algorithms may also have problems to converge.

A segmental multi-point linearization (SML) method was developed to take approximations of the integral expression for the gradient of failure probability in (8) (Liu 2014; Liu et al. 2015). Instead of integrating over the continuous surface, the proposed method fits the limit state surface segmentally with multiple linear pieces, and performs the integration over each piece of hyperplanes. In particular, if we take the first order expansion of the limit state surface at the most likely failure point as single-segmental linear approximation, and perform the integration over this hyperplane, we obtain (9) as a special case. In general, the multi-segmental linear approximation can be written in the following form:

$$\begin{aligned} \nabla_{\mathbf{x}} P_f &= -\int_S \frac{\varphi_n(\mathbf{u})}{\|\nabla_{\mathbf{u}} G\|} \nabla_{\mathbf{x}} G dS \\ &\approx \sum_{j=1}^p W_j \nabla_{\mathbf{x}} G^j \end{aligned} \tag{11}$$

where $\nabla_{\mathbf{x}} G^j$ is the gradient of the limit state function with respect to design variables evaluated at the j th fitting point, which is a point shared by the limit state surface and the corresponding piece of hyperplane. The number of fitting segments is p , so is the number of fitting points, because there is a one to one correspondence. The term W_j is the weight for the corresponding component $\nabla_{\mathbf{x}} G^j$ obtained by integrating (8) over the corresponding hyperplane segment.

The idea of using piece-wise linear segments to approximate nonlinear limit state surface has been used in the literature for approximating failure probability but not for sensitivity analysis. In reference (Ditlevsen and Madsen 2007), the so-called multi-point FORM (also named as polyhedral approximation) adopts locally most central points to construct a tangent bounding polyhedron of the limit state surface. For the version of SML addressed in this paper, instead of bounding the limit state surface with a tangent polyhedron, the method approximately fits the limit state surface with an orthogonal “box”, which leads directly to an easy-to-compute approximation of the sensitivity of failure probability. In addition, the fitting points in our method can be found easily in a systematic way, while in the multi-point FORM, finding local most central points can be a heavy task. In terms of computational cost, the simplified orthogonal fitting scheme only requires solving several 1D nonlinear equations, which is significantly faster than the iterative procedures for searching the local most central points (Kiureghian and Dakessian 1998).

The approximation of $\nabla_{\mathbf{x}}P_f$ by the proposed SML method involves two main steps: (1) selection of fitting points; (2) computation of the weights based on a local linearization of limit state surface around the fitting points.

There are several guidelines for choosing the fitting points. First, since (8) is a surface integral, the fitting points should be on the surface. Second, the fitting points should be close to the origin of the \mathbf{u} -space due to the fact that the low probability density region has little contribution to the integration of (8), which is an effect of the exponential decay of $\varphi(\mathbf{u})$ in the standard normal space. Additionally, the sample points should not be too close to each other in order to avoid repetitive information (i.e., maximize the information content from the selected points/hyperplanes), because in our assumption, there should be no jump in the limit state function, and both $\nabla_{\mathbf{x}}G$ and $\nabla_{\mathbf{u}}G$ should vary smoothly. We proposed several fitting schemes that follow these guidelines as reported in the paper (Liu et al. 2015), namely tangent fitting, step fitting and orthogonal fitting. In this paper, we will use a fitting scheme that is a simplified version of the orthogonal fitting scheme. The proposed simplified orthogonal fitting scheme is particularly tuned for RBTO problems where the limit state functions are generally smooth and have orders lower or equal to two with respect to random variables. In general, it is good for limit state surfaces with smooth and relatively uniform curvatures within the central region of the transformed random space. An example of such smooth limit state function is the compliance of structure with respect to the magnitude of loads. The simplified scheme to find the fitting points for the purpose of RBTO is summarized as follows:

- (1) Select a reference point $\mathbf{u}_{(+1)}$;
- (2) Rotate the coordinate frame such that the reference point lies on the positive half of the first axis of the new coordinate frame;
- (3) Search for intersection points of the new axes and the limit state surface within radius $r = k\tilde{\beta}$ from the origin, where k is a user defined parameter and $\tilde{\beta} = \|\mathbf{u}_{(+1)}\|$.
- (4) Finally the effective fitting points are taken as the intersection points including the reference point.

The rotation of coordinate frame is achieved by a constant orthogonal transformation \mathbf{R} such that $\mathbf{u}'_{(+1)} = \mathbf{R}\mathbf{u}_{(+1)} = [\|\mathbf{u}_{(+1)}\|, 0, \dots, 0]^T$. The rotational matrix \mathbf{R} can be computed by replacing the first column of an identity matrix by $\mathbf{u}_{(+1)}/\|\mathbf{u}_{(+1)}\|$ and applying a QR factorization to the matrix, for example, a Gram-Schmidt process (Heath 1997). We denote the positive direction of the new axes i as $\mathbf{e}'_{(+i)}$ and the negative one as $\mathbf{e}'_{(-i)}$. The

computation of the intersection points can be done by solving 1D nonlinear equations. The solution of these equations can be easily obtained, for example by means of the bisection method (Heath 1997). If for one direction there is no intersection point inside the hypersphere with $r = k\tilde{\beta}$, we take the intersection point to infinity and it is not an effective fitting point. For example, point $\mathbf{u}_{(+2)}$ in Fig. 3 is not an effective fitting point and it is taken to be at the infinity of direction $\mathbf{e}'_{(+2)}$. The parameter k defines how large the search region is. Typically, values should be between 2 and 5 to make the fitting points neither too far nor too close to the origin, such that the nonlinearity of the limit state surface is properly captured.

To determine the weights, the limit state surface is first linearized at the fitting points such that it is approximated by several segments of orthogonal hyperplanes. Suppose the j th effective fitting point is on the positive direction of axis i and it is denoted as $\mathbf{u}^j = \mathbf{u}_{(+i)}$. The hyperplane determined by $\mathbf{u}_{(+i)}$ has a prescribed normal in the direction of $-\mathbf{e}_{(+i)}$. The gradient with respect to \mathbf{u} of the affine function that describes the hyperplane is defined as $\nabla_{\mathbf{u}}G^j\mathbf{e}'_{(+i)}$, which is the projection of the gradient of the limit state function at the corresponding fitting point onto the prescribed normal direction of the hyperplane segment, i.e., $-\mathbf{e}_{(+i)}$. Graphically, the approximation looks like fitting the limit state surface with a “box”. The “box” is shaded in Fig. 3 with dashed boundaries, which are the hyperplane segments. The limit state function is linearized not only with respect to random variables \mathbf{u} but also design variables \mathbf{x} at the fitting points. Therefore, on each hyperplane, $\nabla_{\mathbf{u}}G$ and $\nabla_{\mathbf{x}}G$

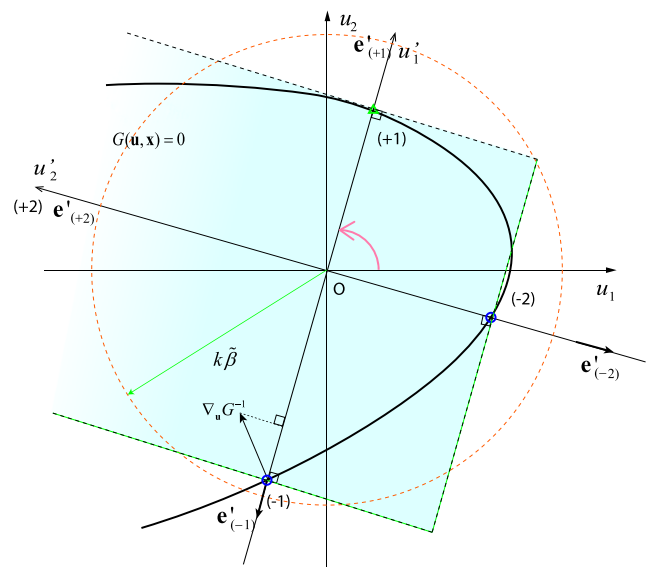


Fig. 3 Graphical illustration of the proposed segmental multi-point linearization method (SML). Green triangle refers to the reference point, blue circles refer to other fitting point, $(\pm i)$ representing $\mathbf{u}_{(\pm i)}$

remain constant. This segmental linearization leads to the following weighted sum:

$$\begin{aligned} \nabla_{\mathbf{x}} P_f &= - \int_S \frac{\varphi_n(\mathbf{u})}{\|\nabla_{\mathbf{u}} G\|} \nabla_{\mathbf{x}} G dS \\ &\approx \sum_{j=1}^p \int_{S_j} - \frac{\varphi_n(\mathbf{u})}{\|\nabla_{\mathbf{u}} G\|} \nabla_{\mathbf{x}} G dS_j \\ &= \sum_{j=1}^p - \frac{\int_{S_j} \varphi_n(\mathbf{u}) dS_j}{\|\nabla_{\mathbf{u}} G^j \mathbf{e}'_{(+i)}\|} \nabla_{\mathbf{x}} G^j \end{aligned} \tag{12}$$

where S_j is one piece of the hyperplane segments, which appears as a facet of the “box”, and p is the number of effective fitting points. Based on (11), we can find the weight for a discrete component $\nabla_{\mathbf{x}} G^j$ as:

$$W_j = - \frac{\int_{S_j} \varphi_n(\mathbf{u}) dS_j}{\|\nabla_{\mathbf{u}} G^j \mathbf{e}'_{(+i)}\|} \tag{13}$$

Then the only task left is to carry out the integral term in (13). Using orthogonality between adjacent planar segments and rotational symmetry of the standard normal space, we obtain:

$$\begin{aligned} \int_{S_j} \varphi_n(\mathbf{u}) dS_j &= \varphi(\|\mathbf{u}_{(+i)}\|) \int_{S'_j} \varphi_{n-1}(\hat{\mathbf{u}}') dS'_j \\ &= \varphi(\|\mathbf{u}_{(+i)}\|) \prod_{k=1, k \neq i}^n (\Phi(\|\mathbf{u}_{(+k)}\|) \\ &\quad + \Phi(\|\mathbf{u}_{(-k)}\|) - 1) \end{aligned} \tag{14}$$

where S'_j is the hyperplane piece S_j described in the rotated coordinates; n is the dimension of random space (i.e. number of transformed random variables). Here \prod refers to the product operator. If $\mathbf{u}_{(\pm k)}$ is not an effective fitting point, we take $\Phi(\|\mathbf{u}_{(\pm k)}\|) = \Phi(\infty) = 1$. Substituting (14) into (13), the weight is given by:

$$\begin{aligned} W_j &= - \frac{\varphi(\|\mathbf{u}_{(+i)}\|)}{\|\nabla_{\mathbf{u}} G^j \mathbf{e}'_{(+i)}\|} \prod_{k=1, k \neq i}^n (\Phi(\|\mathbf{u}_{(+k)}\|) \\ &\quad + \Phi(\|\mathbf{u}_{(-k)}\|) - 1) \end{aligned} \tag{15}$$

The selection of the reference point has some flexibility. Generally, the reference point should be close to the origin in the standard normal space where the probability density is high. Thus the design point, as defined in (10), is suggested to serve as the reference point. The effort of finding the design point is a constrained optimization problem. Researchers have already developed algorithms particularly for this problem, for example the HLRF algorithm (Hasofer and Lind 1973). The improved HLRF algorithm was proposed by Zhang and Kiureghian (1995), which is used in this paper. Because the sensitivity is calculated by combining the information from multiple points, the approximation

is not particularly sensitive to the location of the reference point. Thus usually it is fine to set a relatively high convergence tolerance for the improved HLRF algorithm to save computational resource. More generally, the selection is not restricted to the design point. Sometimes it is beneficial for the accuracy to specify a particular direction for the reference point, and search for the point on the limit state surface along that specified direction (Liu et al. 2015).

Requiring no additional processing, the computed weights can also be used to improve the approximation of P_f . The idea here resembles the multi-point FORM. Consistently with the “box” approximation of the limit state surface, the region inside the “box” can approximate the safe domain as shown in Fig. 3. Due to the orthogonality between adjacent linear segments, the failure probability is approximated by

$$P_f = 1 - \prod_{i=1}^n (\Phi(\|\mathbf{u}_{(+i)}\|) + \Phi(\|\mathbf{u}_{(-i)}\|) - 1) \tag{16}$$

If the design point is taken as the reference point, the above expression can be regarded as an update of P_f approximated by FORM. The obtained P_f will be either larger or equal to the P_f obtained by FORM because we are actually adding more regions to the FORM approximated failure domain in this process. When compared to FORM-based methods, the additional computational cost of SML relates to the search of fitting points and the evaluation of the limit state function and its gradient with respect to design variables. Among them, the calculation of the gradient contributes the most. Because the number of fitting points is no more than $2n$, the computational cost spending in the computation of gradient increases to no more than $2n$ times, with respect to a FORM-based approach.

A physical interpretation of the proposed method in the context of RBTO is that, the method adaptively finds multiple important design cases at each iteration of the topology optimization, and the obtained gradient resembles a weighted sum of the updating information collected from all design cases. If only the loads are considered as random variables, the analogy is the multi-load case topology optimization. This also explains why the obtained structures are not fully stressed designs (Rozvany et al. 1993). Comparing to conventional multi-load case topology optimization, the load cases and their weights are determined by reliability analysis, thus, we are able to control the desired level of reliability of the design. In addition, we can also consider other

variabilities in design condition, such as the randomness of material properties, without having extra difficulty.

4 Formulation of reliability-based topology optimization

The mathematical formulation of the RBTO problem considered in this paper is stated as follows:

$$\begin{aligned} \min_{\mathbf{x}} \quad & V = \mathbf{L}^T \mathbf{x} \\ \text{s.t.} \quad & P(C^{max} - C(\mathbf{x}) < 0) - P_f^t \leq 0 \\ & \mathbf{x}_{min} \leq \mathbf{x} \leq \mathbf{x}_{max} \end{aligned}$$

where \mathbf{L} is a vector of element lengths, and the design variables \mathbf{x} are member areas of the ground structure. The objective is the minimization of the volume of the material used in the structure. Here the limit state function considers an upper bound C^{max} on the total compliance of the structure. The probability of the exceedance of C^{max} is constrained by P_f^t , the target failure probability.

The nested formulation for minimization of volume with compliance constraint on ground structures (Christensen and Klarbring 2008) is used as a foundation to build up the RBTO formulation. The generation of ground structure on structured grid is shown schematically in Fig. 4. In the nested formulation, the state variables \mathbf{d} are explicitly solved using the equation $\mathbf{K}(\mathbf{x})\mathbf{d} = \mathbf{F}$ from finite element analysis. The parameters \mathbf{x}_{min} and \mathbf{x}_{max} are the lower and upper bounds of member areas. A small value ϵ is assigned to \mathbf{x}_{min} in order to prevent singularity of the stiffness matrix \mathbf{K} (Christensen and Klarbring 2008). The RBTO approach is developed in the manner of RIA, where we directly treat the probability constraint in the optimization. The sensitivity of the probabilities in the constraint function is calculated using the SML method as described in Section 3. The optimal topology is extracted using a cutoff strategy: members with cross-sectional areas $x_i < \eta x_{max}$ after optimization are ignored in the output topology, where η is a user-defined parameter to control the level of detail in the print-out of the final topology. Therefore, the presented topologies after the cutoff should only be used to identify the most important components of the optimized truss structures, and do not necessarily reflect stand-alone structures that are locally and globally stable and in equilibrium. However, the traditional ground structure approach is a well-developed method that

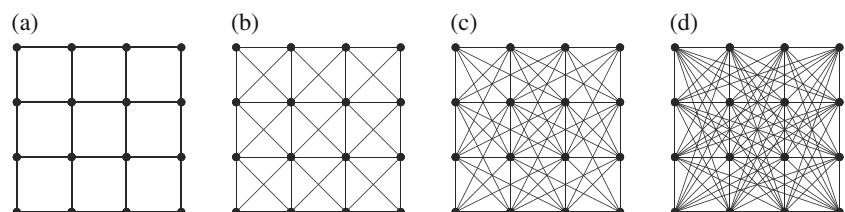
has been shown to successfully indicate the optimal topologies of structures (Bendsøe and Sigmund 2003; Christensen and Klarbring 2008), which serves our primary interest of this paper very well. Ongoing Research aims to improve the traditional sizing approach of ground structure such that one can obtain a stand-alone structure in the end, for example, by applying filter during the optimization (Ramos Jr. and Paulino 2016). However, such considerations are beyond the scope of the present work.

Compliance is defined as $C = \mathbf{F}^T \mathbf{d}$, where \mathbf{d} is the vector of nodal displacement. In linear elastic analysis of structures, compliance is the reciprocal of stiffness. That is, if the compliance is small, the structure is stiff. We use compliance as the limit state for several reasons. First, it gives a global assessment of the structural behavior, such that the optimization formulation becomes mathematically simple and computationally convenient. Second, since compliance is a popular measure in the field of topology optimization, then the comparison between RBTO and deterministic optimization is familiar to readers in that field. Finally, the use of compliance as limit state function preserves the convexity of the original deterministic formulation in certain cases. Given that the volume function and box constraints are convex about the design variables, the convexity of the formulation depends on the convexity of the feasible set defined by the probability constraint. According to Prékopa (1995), a probability constrained feasible set is convex if the following conditions hold:

- (1) the original random variables has continuous log-concave PDF;
- (2) The limit state function is quasi-concave with respect to both design and random variables.

Many probability distributions are log-concave, for example, multivariate normal distribution and exponential distribution. In our case, compliance is a known convex function of the design variables as member areas (Christensen and Klarbring 2008). Because the compliance can be written as a quadratic form of the forces as $C = \mathbf{F}^T \mathbf{K}^{-1} \mathbf{F}$ and \mathbf{K}^{-1} is positive definite, it is also convex about the forces. As the compliance appears in the limit state function with a negative sign, the convexity of compliance indicates the concavity of the limit state function. Therefore, if the random variables are forces with multivariate normal distributions, which is quite common and practical, the

Fig. 4 Ground structure connectivity level generation example on a structured grid. **a** Base 4×4 grid. **b** Level 1 connectivity. **c** Level 2 connectivity. **d** Level 3 connectivity, which is also full connectivity for this grid



probabilistic constraint about compliance forms a convex feasible set. As a consequence, the optimization becomes convex and the solution is guaranteed to be globally optimal. However, this cannot hold as a general conclusion.

We would like to point out that the SML-based RBTO method is neither limited to the ground structure approach nor to the use of compliance as the limit state function. For instance, similar problems could be solved using density-based approaches (Bendsøe and Sigmund 2003).

5 Numerical examples

In this section, we present several numerical examples to demonstrate the validity and features of the proposed method. All of the problems follow the formulation in Section 4. We set $\epsilon = 10^{-5}$. The values of C^{max} , η and P_f^t vary for different problems. In the analyses of the optimized structures, the members being ignored in the output topology are still included to prevent singularity of the stiffness matrices, which have very little influence on the global behavior of the structure (i.e., the global compliance). Without loss of generality, no physical units are adopted, but we ensure that the quantities are consistent in magnitude.

The optimizer used in the examples is the Method of Moving Asymptotes (MMA) (Svanberg 1987), one of the most popular optimization algorithms for structural optimization. In our implementation, as we tune the parameters to achieve and improve convergence, we finally found best performance when the lower asymptote is equal to 0, which makes the optimizer become equivalent to the Convex Linearization method (CONLIN) (Fleury and Braibant 1986). The algorithm of CONLIN is now rarely used in topology optimization because of its slow convergence, which is a result of the over conservative convex approximation (Christensen and Klarbring 2008). However, for the RBTO problems considered in this research, a conservative approximation is indeed preferred. One of the reasons is that RBTO usually involves updates in both design space and random space at each iteration step. If the design variables change too fast, the reliability analysis may not be able to

correctly capture the change of limit state surface in the random space. For more details regarding the implementation of the optimizer, the readers are referred to the reference (Liu 2014).

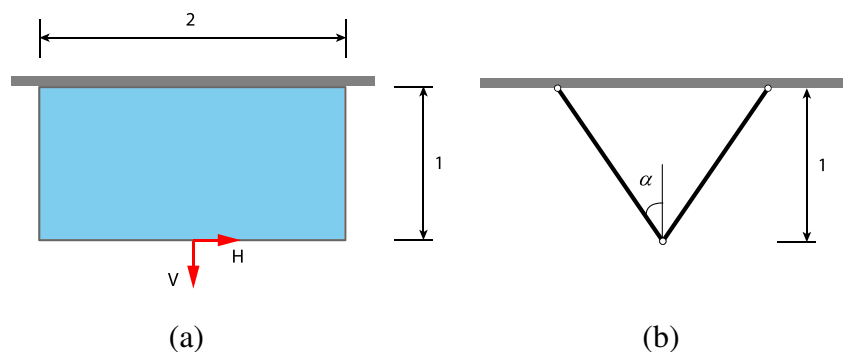
In the examples, in addition to the reliability index $\beta = \Phi^{-1}(R)$, we also provide the value of corresponding reliability R . To evaluate the accuracy of the probability approximation by the SML method, we need to use the value of reliability directly rather than the reliability index, which is obtained by a logarithm-like transformation of the reliability (Rackwitz 2001).

5.1 A benchmark problem

The first example is a benchmark problem for RBTO proposed by Rozvany (2008) and Rozvany and Maute (2011). The analytical solution for the problem has been derived, so it can be used to check the validity of numerical methods for RBTO. The problem is depicted in Fig. 5a. The design domain has width $L = 2$ and depth $D = 1$, and is pinned along the whole upper boundary. The horizontal force H is the only random variable, which is characterized by a standard normal distribution with a mean of zero and a standard deviation of one. The vertical force V is fixed with a value of 3.0 acting downwards. Young's modulus E is taking a unit value. The threshold for the compliance is set to be $C^{max} = 1$. The target failure probability is 0.0027, which corresponds to a desired reliability index $\beta^t = 2.7822$ (i.e., failure probability $P_f^t = 0.0027$), according to reference (Rozvany 2008).

The problem can be transformed equivalently to a deterministic multi-load case topology optimization problem for two cases that $H = \pm 3.0$ (Rozvany 2008; Rozvany and Maute 2011), which was solved analytically in (Rozvany et al. 1993). Then based on the solution for the equivalent deterministic multi-load case problem, the analytical solution of the RBTO benchmark problem is given by a two-bar truss as shown in Fig. 5b with $\alpha = 35.264^\circ$. The minimum volume of the truss is $Vol = 60.75$. The reliability of the optimal design is calculated by integrating the PDF of the normal distribution of the random variable H from -3

Fig. 5 Benchmark problem for RBTO. **a** Domain, loading and boundary conditions. **b** Analytical solution for the optimal topology, where $\alpha = 35.264^\circ$ and $Vol = 60.75$



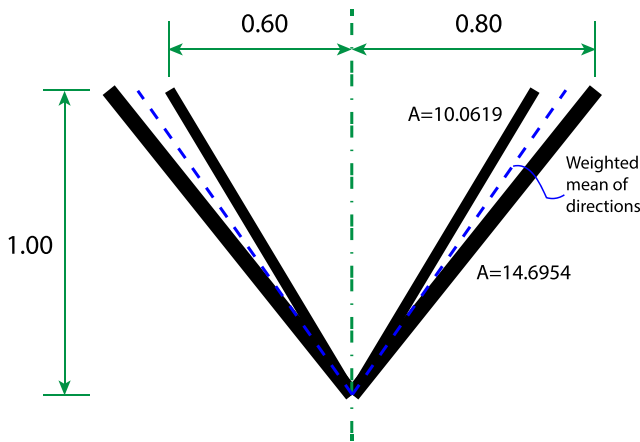


Fig. 6 The optimized topology by the proposed SML-based RIA based on a 11×6 grid ground structure

to 3, the interval that is essentially the safe domain of the structure in the random space. Therefore, the reliability is $R = 2\Phi(3) - 1 = 0.9973$, which achieves the target.

Typically, numerical approaches based on FORM cannot solve this problem since there are actually two design points for a symmetric structure that the solution should be (i.e. $u_1^* = -3.0$ and $u_2^* = 3.0$), thus the FORM approximated gradient always ignores one of the two scenarios. For this problem, the inverse reliability analysis involved in PMA can actually be solved analytically. Thus numerical implementation in reference (Rozvany and Maute 2011) using this idea successfully reproduced the analytical solution. However, for most practical problems, an analytical solution for the inverse reliability analysis cannot be derived easily. A more general numerical approach that can solve this problem correctly is desired.

The proposed approach shows its capability solving the benchmark problem. The numerical solution is first extracted from a 11×6 ground structure grid, with full connectivity between nodes in order to sweep the maximum solution space. Due to the discrete nature of the

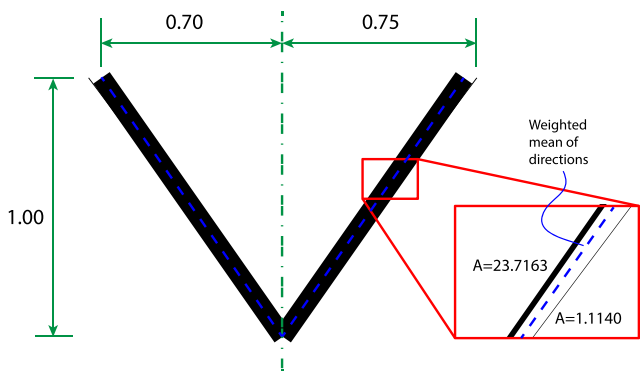


Fig. 7 The optimized topology by the proposed SML-based RIA based on a 41×2 grid ground structure

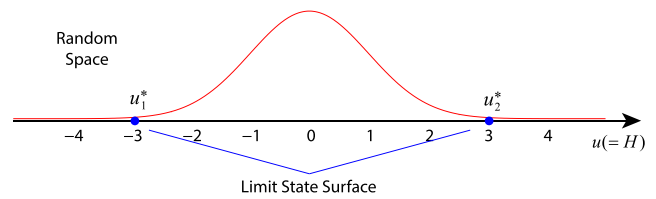


Fig. 8 The random space for the benchmark problem, where $u = H$ since no transformation is needed. The red curve plots the probability density function of u

ground structure, the optimized topology after the cutoff with $\eta = 0.01$ actually consists of four bars as shown in Fig. 6. The value of the final objective is $Vol = 61.3783$, 1.03 % larger than the analytical optimal volume. By taking weighted averages of the orientations of each pair of the bars with respect to member areas, the interpolated two-bar layout turns out to be very close to the analytical solution with $\alpha = 35.698^\circ$, at a difference of 1.23 %. This linear interpolation strategy is adopted from the reference (Rozvany et al. 1993). It is expected that a four-bar truss is obtained, because the ground structure approach searches for the projection of the optimal solution in the limited solution space, and there is no pair of bars that has the exact orientations as the analytical solution in our ground structure. This issue can be diminished by refining the ground structure. Since the first example already shows that the solution consists of 4 straight bars, to save computational cost, a 41×2 grid with full connectivity is used as the refined ground structure, which has 1761 non-overlapping potential members. The obtained topology from the new ground structure is shown in Fig. 7. The two thin bars of the 4-bar truss, although are still above the cutoff limit, are almost negligible since their member areas are just 4.70 % of the thick bars. The weighted mean value of the bar direction gives $\alpha = 35.078^\circ$ and the total volume of the final design is $Vol = 60.9092$. The differences in the volume and angle to the analytical solutions are 0.26 % and 0.53 %, respectively. If we increase the cutoff limit η to neglect the two slender bars, the two thick bars orient to the angle of 34.992° , which still agrees well with the analytical solution.

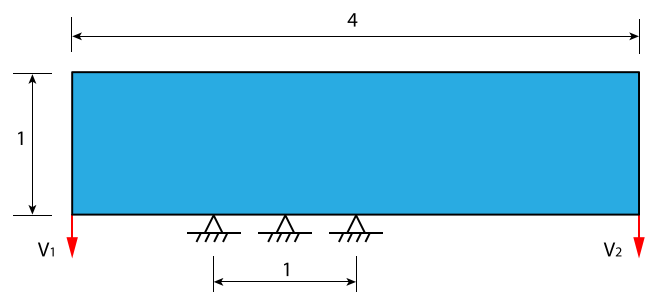


Fig. 9 Design domain and boundary condition of the asymmetric crane arm design

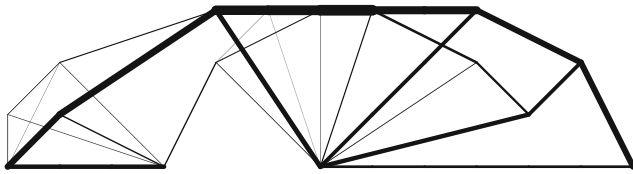


Fig. 10 Optimized topology by deterministic topology optimization

Using our approach, without any knowledge of the problem a priori, we can actually make the KKT conditions satisfied exactly at the optimal solution. This is due to the fact that for this single random variable problem, the limit state surface becomes just two points as shown in Fig. 8. The proposed method is able to find these two points and the approximation of the limit state surface becomes exact, hence the computed $\nabla_{\mathbf{x}}P_f$ and P_f become exact in the given design spaces (i.e. the ground structures). Symmetry of the structure is not imposed before optimization, however, by directly solving the probability constrained optimization with the accurate evaluations of $\nabla_{\mathbf{x}}P_f$ and P_f , we are able to converge to the symmetric analytical solution, even if we start the optimization from asymmetric initial designs. This also verifies the correctness of the analytical solution for this RBTO benchmark problem.

5.2 Crane arm design

This example demonstrate the advantages of the proposed method by comparing the results of deterministic topology optimization, FORM-based RBTO and the proposed SML-based RBTO. The PMA is performed as an example of the FORM-based RBTO algorithms. The objective of this problem is to find an optimal topology for the structural design of a crane arm, which is a 2D beam loaded at its two ends with supports in the middle. The design domain is a 4×1 rectangle box (see Fig. 9). The material of the structure is linear elastic with Young's Modulus $E = 100$. The structure is pin-supported along a unit length portion of the bottom, starting from 1 to 2 in distance from the very left end. Two independent vertical loads V_1 and V_2 are acting on the two bottom tips of the beam. Thus the boundary condition is not symmetric. Each of the forces is assumed to follow a normal distribution with a mean of 7.0 and a standard deviation of 3.0. Thus the coefficients of variation are then around 0.43,

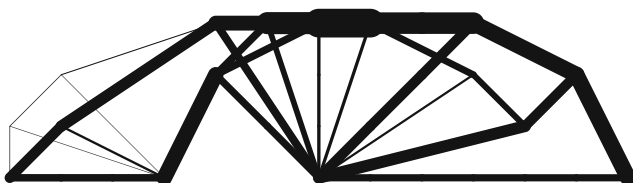


Fig. 11 Optimized topology by FORM-based PMA

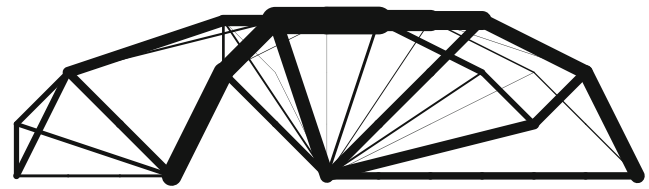


Fig. 12 Optimized topology by SML-based RIA with design point as the reference point

indicating relatively large variability of the forces around their mean values. The target reliability index is set to be $\beta^t = 2.0$ ($R^t = 0.9772$). The limit on compliance is set to be $C_{max} = 1.2$. The settings are rather arbitrary, as they are only used to show the general applicability of the proposed method. A constant cutoff parameter $\eta = 0.02$ is applied throughout this example. Since there are only two random variables involved, we can plot the limit state surface in 2D in order to illustrate how the SML method works in detail. The ground structure used to do the optimization is based on a 13×4 uniform grid with level 6 nodal connectivity, which contains 629 non-overlapping members.

The optimized topology by deterministic approach, after the cutoff being applied, is shown in Fig. 10, where the variations of loads are not considered. We define the deterministic problem using the mean values of the random variables. If the obtained structure is actually subjected to

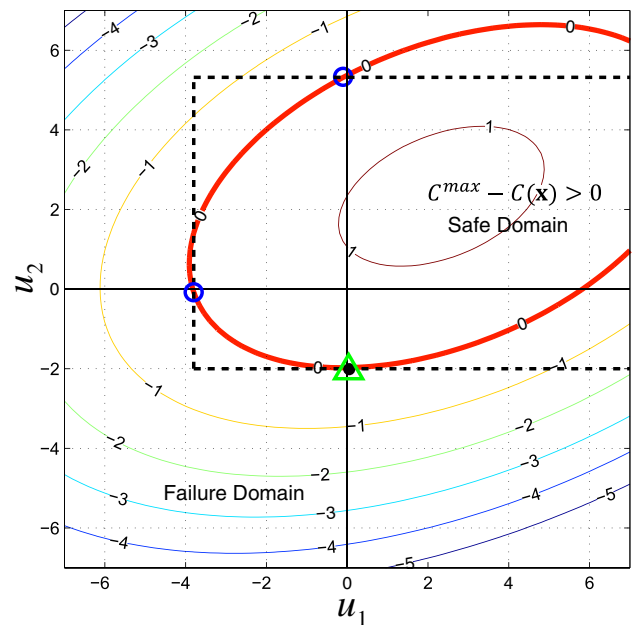


Fig. 13 Contour plot of limit state function for the optimized design in Fig. 12. The blue circles indicate the fitting points; the green triangle refers to the reference point; the black dot is the design point; the red solid curve is the limit state surface. The real limit state surface (red solid curve) is closed, but the approximated limit state surface (black dashed lines) is not, because the fourth intersection point is not an effective fitting point

Table 1 Summary of optimization results by different approaches

Approach	Vol	β_{MCS} (R_{MCS})	cutoff η
Deterministic	85	1.04 (0.8508)	0.02
FORM-based PMA	274	1.51 (0.9345)	0.02
SML-based RIA	278	1.91 (0.9719)	0.02

random loads, the reliability of the structure is measured using MCS with a convergence criterion of 2.5 % coefficient of variation (*c.o.v.*). The MATLAB function for MCS included in the FERUM package (Hahnel et al. 2000) is used in this example and will be used in the remainders of the section. Figure 11 shows the result obtained by the FORM-based PMA. Finally, by setting the design point as the reference point in the embedded SML subroutine, the SML-based RIA provides an optimized topology as shown in Fig. 12 after the cutoff. The actual reliability of the optimized structures by FORM-based and SML-based methods are also measured by MCS after the optimization, since the target reliability is achieved in an approximate way for both approaches. The contour plot of the limit state function of the design obtained by the SML-based method is shown in Fig. 13. The reference point generates 3 fitting points in total including itself. The design point corresponds to the critical scenario when $V_1 = 7.2838$ and $V_2 = 13.0210$.

Table 1 compares the numerical results of the three structures. The analytical solution is not known for this problem, but we can conclude that the design by SML-based RIA (as shown in Fig. 12) is more favorable than the design by FORM-based method. The two designs are almost the same in volume, but the design by the new approach has a higher actual reliability as measured by MCS, which means that the material is assigned more efficiently by the proposed algorithm than the conventional FORM-based algorithms. *This comparison illustrates the problem of FORM-based methods as discussed in Section*

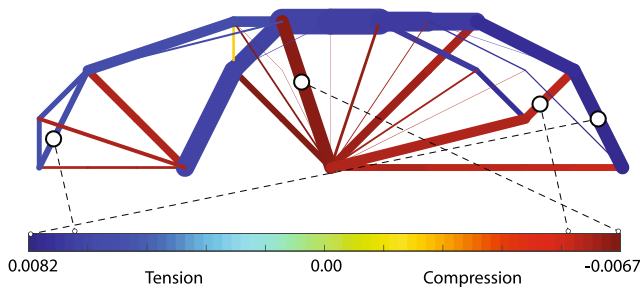


Fig. 14 Stress distribution in the optimized topology after cutoff. Different colors refer to different values of stress in the members

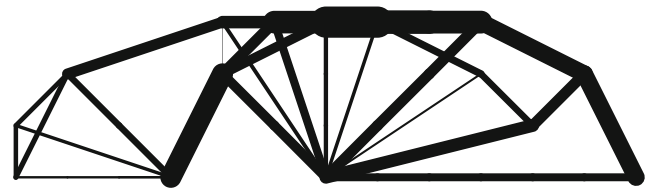


Fig. 15 Optimized topology by SML-based RIA considering randomness of E

1, which is that, mainly due to the error in the first order approximation of the sensitivity, they might not converge to a solution as close to an optimum as the one obtained by the proposed approach. Typically, FORM-based methods would converge to an optimized design corresponding to a single design case. On the contrary, the SML-based method converges to designs that corresponds to multiple design cases. Therefore, optimized structures by the SML-based approach are more reliable in general than the ones obtained by FORM-based approaches. We would like to remark that the design obtained by SML-based RBTO is not a fully stressed design. The volume-compliance formulation for topology optimization is known to converge to fully stressed designs under single load case (Christensen and Klarbring 2008). The full stress referred here is not a physical constraint in the formulation, but rather an analytically derived uniform stress value for all members in the optimized topology depending on the Lagrange multiplier for the constraint about compliance (Christensen and Klarbring 2008). As mentioned before, the SML-based RBTO design

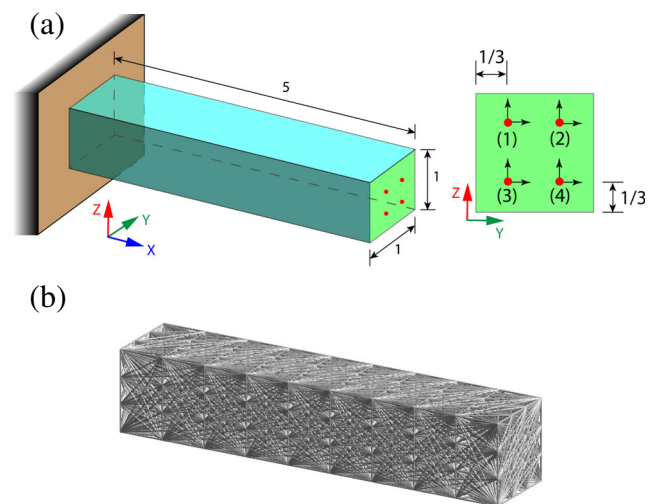


Fig. 16 a Design domain and boundary conditions; b Initial ground structure generated on a 10x4x4 grid with level 3 connectivity, which contains 6400 non-overlapping bars

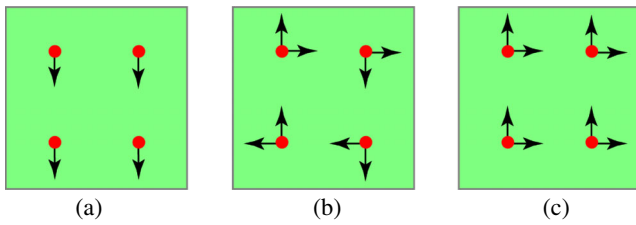


Fig. 17 Possible loading scenarios. **a** Bending in Z direction; **b** Twist of the cantilever; **c** Bending in Y-Z direction

is naturally similar to a multi-load case design, and for a structure optimized for multiple load cases, it is impossible to be fully stressed under any single load case. Figure 14 depicts the stress distribution in the structure under the load case given by the design point (i.e., $V_1 = 7.2838$ and $V_2 = 13.0210$). Members with areas lower than the cut-off limit are also not shown. We observe that the stresses are not the same for the members in the compression group or in the tension group, thus the structure is not uniformly stressed under the critical load case. However, the members are generally highly stressed, implying that the material still works efficiently. As we measured in this example, the number of calls executing the gradient computation in the SML-based approach is 3.96 times of the FORM-based one. This is because the number of fitting points in this problem is varying from 1 to 4 for different iterations, and most of the time there are 4 fitting points.

Thanks to the generality of the proposed method in dealing with random variables, it is not difficult to incorporate the randomness in material property. We can add the Young’s modulus as an additional random variable

which has a lognormal distribution with a mean of 100 and a standard deviation of 10. The lognormal distribution is employed because it cannot have a negative value, which matches the physical nature of Young’s modulus. The optimal design has $Vol = 286$ and $\beta_{MCS} = 1.90$. Comparing to the design with a fixed E , we observe that the volume increases due to the introduction of randomness in material property. The optimal topology is presented in Fig. 15, which is also slightly different from the one without considering randomness of the Young’s modulus.

5.3 3D cantilever

This example is to demonstrate the ability of the method to handle large variation in loading condition. Here we try to find an optimal topology for a 3D cantilever. The design domain is shown in Fig. 16a. The cantilever is subject to eight forces applied at four points on the right facet of the cantilever, and it is pin-fixed on the left facet. All the eight random forces are uncorrelated and share the same marginal probability distribution: the normal distribution with a zero mean and a standard deviation of 2.0. The limit state function is defined to have a threshold of 5.0 on total compliance. Young’s modulus $E = 100$ is used as material property and is fixed in this problem. The ground structure is generated on a $10 \times 4 \times 4$ grid with level 3 connectivity of nodes leading up to 6400 non-overlapping potential members as shown in Fig. 16b.

In this problem, because the mean values of the random forces are zeros, the solution of the optimization problem is totally defined by the variation of random forces. With the setting of uncertain loads, the structure could have many possible static states. For example, Fig. 17a shows

Fig. 18 Four views of the optimal topology obtained by SML-based RBTO algorithm for $\beta^l = 2.0$. Member sizes are normalized by maximal area $x_{max} = 10.0370$

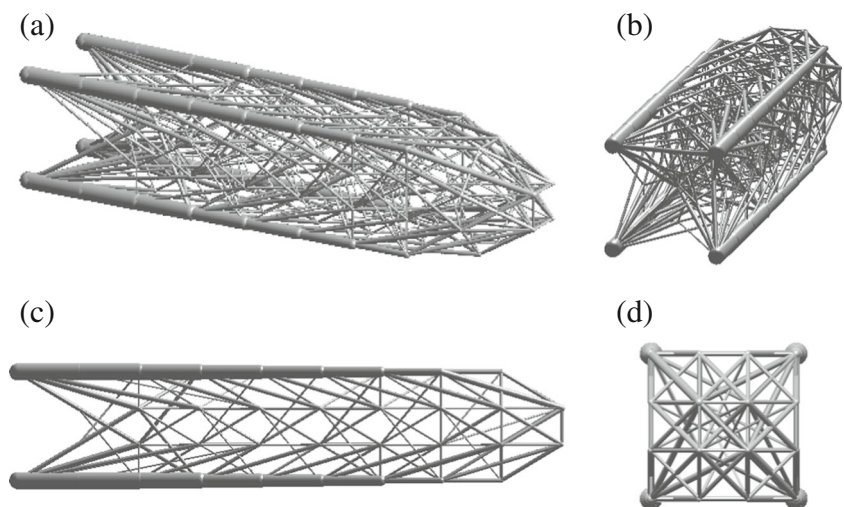
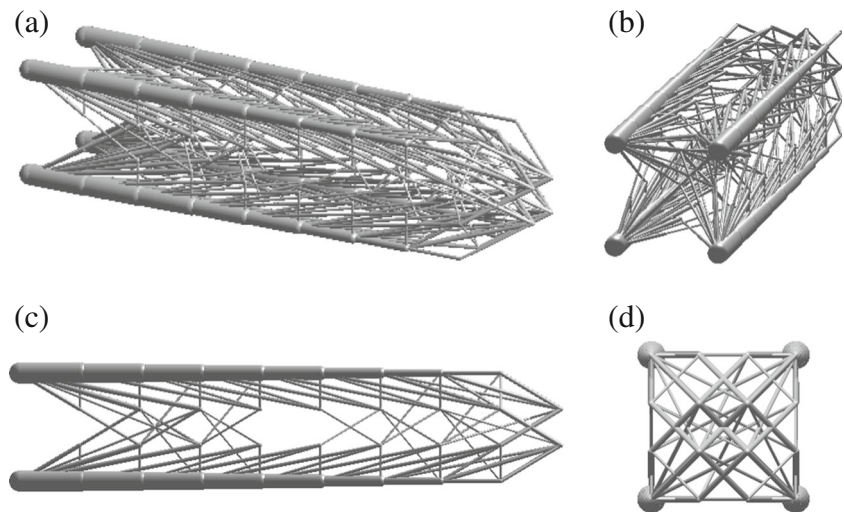


Fig. 19 Four views of the optimal topology obtained by SML-based RBTO algorithm for $\beta^t = 2.5$. Member sizes are normalized by maximal area $x_{max} = 15.3063$



the scenario that the cantilever is subjected to bending in Z direction; Fig. 17b exhibits the scenario when an equivalent torsion is applied to the cantilever; it is also possible that a bending happens along the diagonal direction of Y-Z plane as shown in Fig. 17c. There are still many other possible combinations of forces.

Because this example considers very complicated loading cases, it is difficult to perform FORM-based RBTO design and deterministic optimization as references. As we try the FORM-based PMA for this problem, it diverges quickly. Because RIA is less robust than PMA, we can expect that FORM-based RIA will also diverge. This problem is also difficult to be formulated in a deterministic manner, because the mean values are all zeros. It might be possible to select some typical loading cases, for example the scenarios shown in Fig. 17, and perform optimization

with prescribed multiple loading cases, however, the relative importance of each loading case needs to be specified manually which may not reflect the real reliability of the structure.

Using the proposed SML-based approach, topology optimization solutions are obtained for different target reliabilities as shown in Figs. 18, 19 and 20. The member sizes are shown such that they are proportional to the computed sizes. For each design, four views are shown in order to help recognize the frame layouts. The obtained designs are compared in Table 2. In order to present a clear configuration of the topology, different cutoff criteria are applied to the three cases. In the traditional ground structure approach, this only influences the print-out topologies, and the underlying structures are not affected. We also count the number of bars appear in the shown topologies after the cutoff is applied.

Fig. 20 Four views of the optimal topology obtained by SML-based RBTO algorithm for $\beta^t = 3.0$. Member sizes are normalized by maximal area $x_{max} = 20.6788$

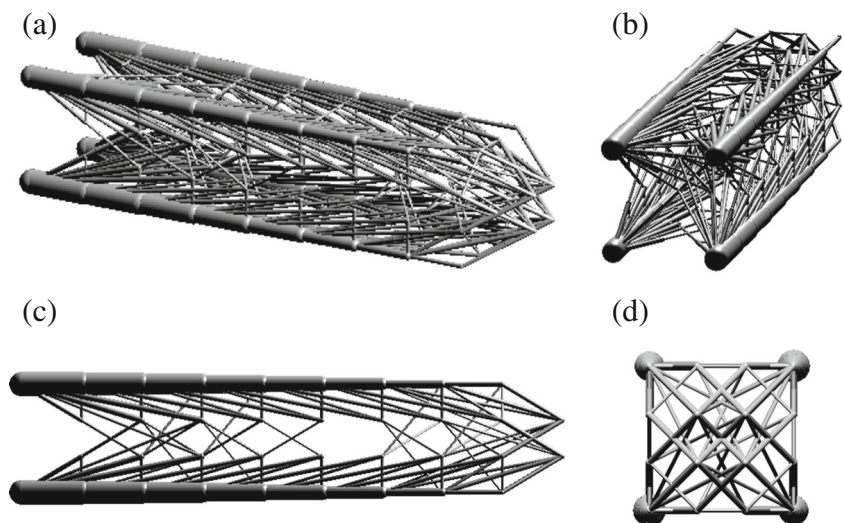


Table 2 Summary of Optimized Structures for Different Target Reliabilities

$\beta^t (R^t)$	Vol	$\beta_{MCS} (R_{MCS})$	cutoff η	Number of Bars
2.0 (0.9772)	232	1.34 (0.9099)	0.015	310
2.5 (0.9938)	345	1.83 (0.9664)	0.010	358
3.0 (0.9987)	478	2.38 (0.9913)	0.010	367

Most of the members are ignored because they are not contributing much to the stiffness of the cantilever structure given the loads. The optimized topologies for the three cases are very similar, but we observe a dramatic increase in optimized volume (i.e., the objective). We also notice that the error in the approximation of failure probability is relatively large in this example, which is partially due to the high dimension of the random space. After all, the performance of the proposed method is still good, as we can identify in the final topologies some classical layout patterns that are good for flexural and torsional stiffness.

5.4 3D tower crane design

The final example is a comprehensive design problem towards potential realistic applications. The structure to be optimized is a tower crane shown in Fig. 21. The structure is attached to the ground by means of displacement restriction conditions. There are 3 vertical loads in Z direction at point (1), (2), and (3) which are denoted as V_1, V_2, V_3 . The 6 horizontal loads in X-Y plane are also applied at the 3 points. They are denoted as $H_{D,i}$, where D is either X or Y direction, indicating the direction of the force, and i refers to the point where the forces are applied. Not only the forces, but also the Young’s modulus is taken as a random variable in this problem. We enforce that $V_1 = V_2, H_{X,1} = H_{X,2}, H_{Y,1} = H_{Y,2}$, hence there are in total 7 random variables.

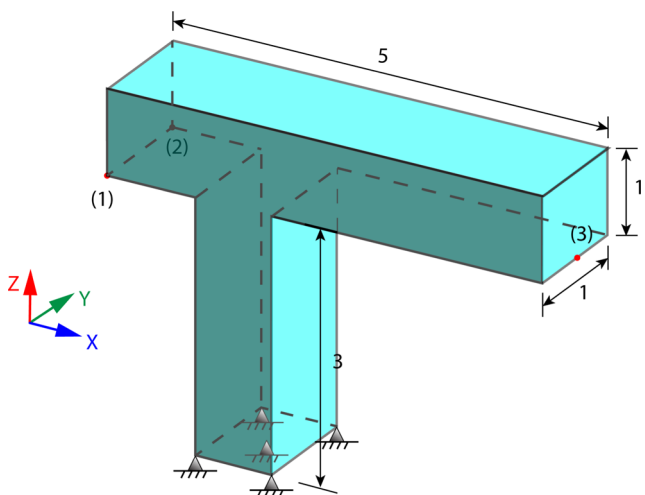


Fig. 21 Design domain and boundary conditions for 3D crane design

The probability distributions of the random variables can be found in Table 3, where μ is the mean value, σ is the notation for standard deviation, and ρ refers to correlation coefficient. To explore the influence of the variation of random variables, we set up two different cases for σ 's. In Case 2 the random variables have the same distributions and means as in Case 1, but the standard deviations are two times larger than in Case 1. Besides, unlike the previous examples, the random variables in this problem are not totally independent of each other, which makes the problem more practical. For the RBTO problem, $\beta^t = 3.0 (R^t = 0.9987)$ for both cases. The threshold of compliance in the limit state function is 5.0. The concave shaped design domain makes the generation of embedding ground structure complicated because we have to avoid bars that across the void region. We use the efficient algorithm developed by Zegard and Paulino (2014, 2015) to do the job. The ground structure used to perform the optimization is then shown in Fig. 22a which has 2620 non-overlapping members.

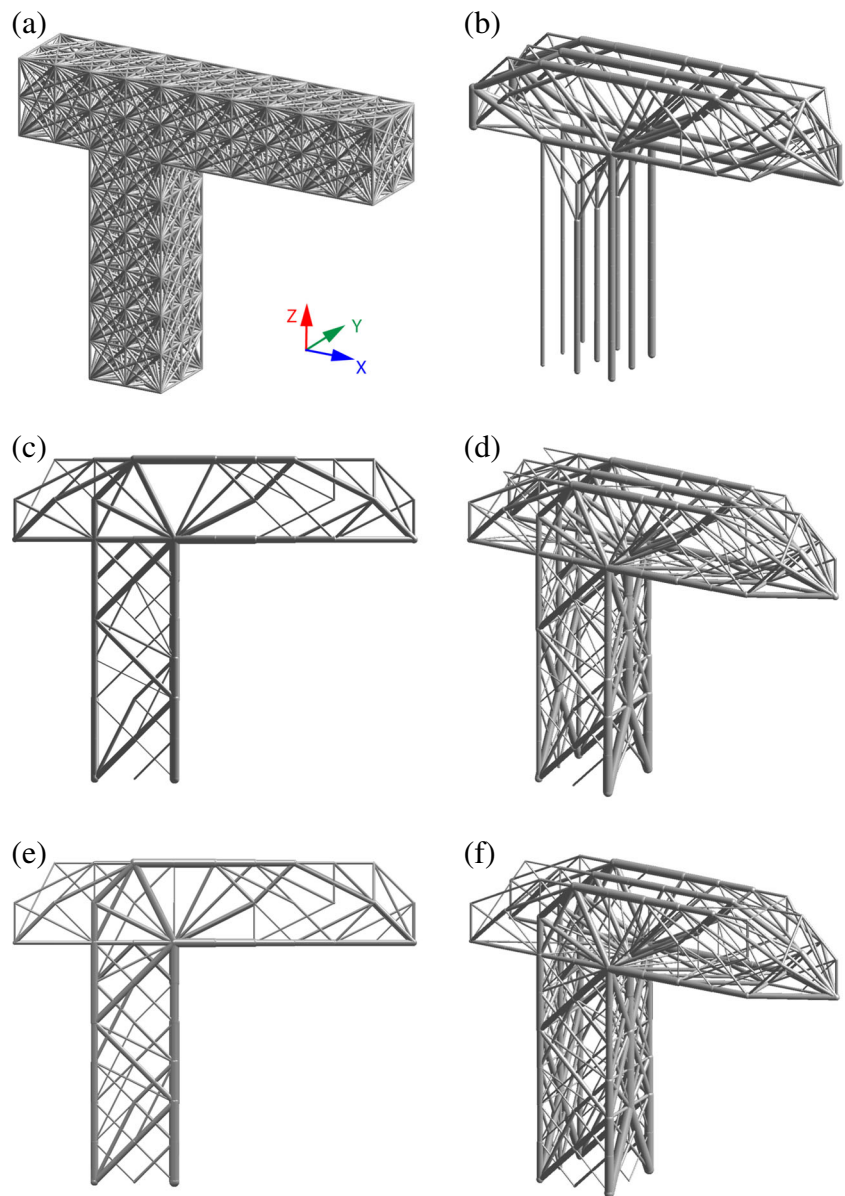
The deterministic topology optimization performed based on mean values provides a topology as shown in Fig. 22b. Figure 22c to f plot two optimized topologies by performing RBTO using the proposed SML-based approach. Members are plotted proportional to member sizes normalized by the maximal area (x_{max}) of each optimized structure.

The optimized design by deterministic topology optimization has a volume equal to 13 which is extremely small and the structure is very sensitive to even a small perturbation in loads. We can identify from the topology that the main components of the lower structure are isolated columns without bracings. Although the actual stiffness matrix of the obtained structure is not singular due to the existence of many extremely slender bars that are neglected after the cutoff, the extracted essential topology indicates that the structure is not reliable and robust to variations in loads. The optimized topology shown in Figs. 22c and d is designed for Case 1 where the random variables have smaller variations. The optimal volume turns out to be 276 and the reliability index measured by MCS is $\beta_{MCS} = 2.56 (R_{MCS} = 0.9948)$. The number of bars in the presented

Table 3 Statistics of Random Variables for 3D Tower Crane Design

Variable	Distribution Type	μ	σ (Case 1)	σ (Case 2)	ρ
$V_1 (= V_2)$	Normal	-3	0.5	1	0.0
V_3	Normal	-3	1.5	3	0.0
$H_{X,1} (= H_{X,2})$	Normal	0	0.5	1	0.3
$H_{X,3}$	Normal	0	1	2	0.3
$H_{Y,1} (= H_{Y,2})$	Normal	0	0.5	1	0.3
$H_{Y,3}$	Normal	0	1	2	0.3
E	Lognormal	100	5	10	0.0

Fig. 22 **a** The ground structure containing 2620 non-overlapping bars. **(b)** Optimized topology by deterministic topology optimization; $x_{max} = 0.3496$. **(c)** Side view and **(d)** isometric view of the optimized topology by SML-based RBTO for Case 1; $x_{max} = 6.2064$. **(e)** Side view and **(f)** isometric view of the optimized topology by SML-based RBTO for Case 2; $x_{max} = 19.4276$



topology is 344 after cutoff using $\eta = 0.015$. The topology shown in Fig. 22e and f considers Case 2 where the random variables have larger variations. The optimized structure has an volume of 879. The reliability index measured by MCS is $\beta_{MCS} = 2.54$, which corresponds to $R_{MCS} = 0.9944$. There are 381 essential members in the shown topology using the same cutoff parameter.

Comparing the results obtained by deterministic topology optimization and RBTO, the optimized topology by RBTO has more redundant members in the structure after cutoff than the deterministic one, as the same cutoff parameter is applied to all cases. Beyond that, it is also observed that the lower structure of the tower crane in the optimized topology by RBTO becomes hollow and has 4 main pillars with lateral bracings around the perimeter, which is

beneficial for flexural and torsional stiffness. The lateral and torsional loads can be introduced by variations of the horizontal forces, which models the wind effects. For the two cases of random variables, no significant difference in the optimized topologies is found, but the volume of material occupied by the optimized structure increases nearly 3 times. This helps to keep the structure still reliable under larger uncertainties, as the magnitudes of forces are more likely to be larger than in Case 1.

The convergence plot for the second case is included in Fig. 23. The blue line shows the convergence of objective function, while the red line shows the estimated value of reliability index of each intermediate design. The estimated β (by the SML method) finally converges to β' , as the probabilistic constraint becomes active. The convergence

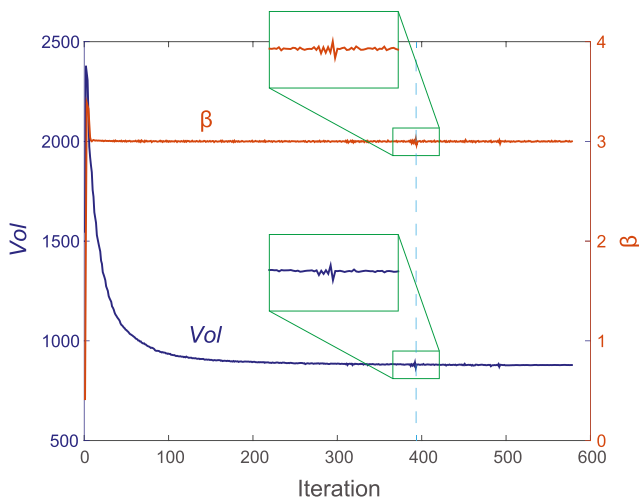


Fig. 23 Convergence plot of the RBTO problem in Case 2. The blue line shows the change of objective during the optimization. The red line shows the change of reliability index (approximated by SML method)

is generally smooth. Although there are small oscillations (as shown in the zoom-in box) during the process, the optimization converges successfully in the end.

6 Conclusion

The random nature and uncertain variation of design condition can affect the favorable design of a structure that is both reliable and economic. To address this concern, reliability-based topology optimization (RBTO) was proposed, which, however, is more challenging to solve than deterministic topology optimization due to the existence of probabilities in the formulation. Numerical approaches for RBTO typically have to take approximations of the probabilities and their gradients, thus the KKT optimality conditions are only approximately satisfied even at a converged numerical solution, excluding rounding errors. The key to get closer to an exact KKT point is to improve the accuracy of the approximations of the probabilities and their gradients.

This paper proposes a gradient-based RBTO approach, which adopts the segmental multi-point linearization (SML) method to improve the estimation of the probability of failure and its gradient with respect to design variables. The SML-based approach is more suitable for RBTO problems with nonlinear limit state functions than conventional FORM-based methods in particular due to the improved accuracy in the estimation of the gradient of the probability with respect to the design variables.

The proposed approach is applied to truss layout optimization problems based on ground structures. Several examples are shown considering uncertainties in loads and

material property. Due to the improved accuracy in sensitivity estimation and reliability assessment, the proposed method can converge to the analytical solution of a benchmark RBTO problem, and at the same time it is applicable to RBTO problems for which analytical solutions are typically not available. In some examples, the SML-based approach is capable of converging to an optimized design that possesses more efficient use of material than the designs by conventional FORM-based methods. In some other examples, the SML-based approach can provide optimized solutions when FORM-based methods fail to converge.

The proposed optimization approach converts to the traditional FORM-based approach automatically when the limit state function is linear or nearly linear if the design point is selected as the reference point in the embedded SML subroutine. As a gradient-based method, the computational efficiency of the proposed approach is also quite attractive.

Acknowledgments We acknowledge support from the US NSF (National Science Foundation) through Grants 1321661 and 1437535. In addition, Ke Liu acknowledges support of the China Scholarship Council (CSC), and Glaucio H. Paulino acknowledges support of the Raymond Allen Jones Chair at the Georgia Institute of Technology. The authors would like to extend their appreciation to Prof. Krister Svanberg for providing a copy of his MMA (Method of Moving Asymptotes) code, and to Dr. Tomas Zegard for providing his 3D plotting subroutine in MATLAB which was used to prepare some of the figures in this paper.

Appendix: Nomenclature

Abbreviations

c.o.v.	Coefficient of variation
CDF	Cumulative Distribution Function
CONLIN	Convex Linearization Method
FORM	First Order Reliability Method
HLRF	Hassofer-Lind-Rackwitz-Fiessler (Algorithm)
KKT	Karush-Kuhn-Tucker (Optimality Conditions)
MCS	Monte Carlo Simulation
MMA	Method of Moving Asymptotes
MPP	Most Probable Point
PDF	Probability Density Function
PMA	Performance Measure Approach
RBDO	Reliability-Based Design Optimization
RBTO	Reliability-Based Topology Optimization
RIA	Reliability Index Approach
SML	Segmental Multi-point Linearization
SORM	Second Order Reliability Method

Symbols

\bar{G}^j The affine function describing hyperplane segment i

\bar{S}_j Hyperplane segments of a piecewise linearized limit state surface
 β Reliability index
 β^t Target reliability index
 $\delta\Omega$ Change of failure domain
 \mathbf{e}_i Orthonormal basis of space
 \mathbf{R} Rotational matrix
 \mathbf{u} Transformed random variables
 \mathbf{u}^* Most likely failure point (design point)
 \mathbf{x} Design variables
 Ω, Ω' Failure domain and failure domain after design update
 Φ, φ CDF and PDF of standard normal distribution
 G Limit state function in transformed random space
 G^e Equivalent limit state function
 h_k Deterministic constraints
 k User defined parameters for the fitting scheme
 n Number of random variables
 p Number of fitting points
 P_f Failure probability
 P_f^t Target failure probability
 R Reliability measured in probability
 R^t Target reliability
 S Limit state surface
 W_j Weight for contribution of segment j

References

- Achtziger W, Bendsøe M, Ben-Tal A, Zowe J (1992) Equivalent displacement based formulations for maximum strength truss topology design. *IMPACT of Computing in Science and Engineering* 4(4):315–345
- Beghini LL, Beghini A, Katz N, Baker WF, Paulino GH (2014) Connecting architecture and engineering through structural topology optimization. *Eng Struct* 59(0):716–726
- Bendsøe M, Sigmund O (2003) *Topology Optimization: Theory, Methods and Applications*. Springer
- Ben-Tal A, Bendsøe M (1993) A new method for optimal truss topology design. *SIAM J Optim* 3(2):322–358
- Breitung K (1991) Parameter sensitivity of failure probabilities. In: Der Kiureghian A., Thoft-Christensen P. (eds) *Reliability and Optimization of Structural Systems 90*, Vol. 61 of *Lecture Notes in Engineering*, Springer Berlin Heidelberg, pp 43–51
- Cheng G, Xu L, Jiang L (2006) A sequential approximate programming strategy for reliability-based structural optimization. *Comput Struct* 84(21):1353–1367
- Choi S, Grandhi R, Canfield R (2006) *Reliability-based Structural Design*. Springer
- Christensen P, Klarbring A (2008) *An Introduction to Structural Optimization*. Springer, *Solid Mechanics and Its Applications*
- Ditlevsen O, Madsen HO (1996) *Structural Reliability Methods*. Wiley
- Ditlevsen O, Madsen H (2007) *Structural Reliability Methods*. Technical University of Denmark
- Fleury C, Braibant V (1986) Structural optimization: A new dual method using mixed variables. *Int J Numer Methods Eng* 23(3):409–428
- Hahnel A, Franchin P, Gencturk B, Song J, Pakzad S, Sudret B, Bourinet J, Haukaas T (2000) *Finite element reliability using MATLAB (FERUM) Version*, vol 3. University of California, Berkeley, California
- Hasofer A, Lind N (1973) *An Exact and Invariant First-order Reliability Format*. Solid Mechanics Division, University of Waterloo
- Heath M (1997) *Scientific Computing: An Introductory Survey*, Second Edition. McGraw-Hill
- Hohenbichler M, Rackwitz R (1986) Sensitivity and importance measures in structural reliability. *Civ Eng Syst* 3(4):203–209
- Jalalpour M, Igusa T, Guest JK (2011) Optimal design of trusses with geometric imperfections: Accounting for global instability. *Int J Solids Struct* 48(21):3011–3019
- Kiureghian AD, Dakessian T (1998) Multiple design points in first and second-order reliability. *Struct Saf* 20(1):37–49
- Liang J, Mourelatos ZP, Nikolaidis E (2007) A single-loop approach for system reliability-based design optimization. *Impact of Computing in Science and Engineering* 129(12):1215–1224
- Liu K (2014) *Segmental multi-point linearization for topology optimization and reliability analysis*. Master's thesis, University of Illinois, USA
- Liu K, Paulino GH, Gardoni P (2015) Segmental multi-point linearization for parameter sensitivity approximation in reliability analysis. *Struct Saf*
- Mathakari S, Gardoni P, Agarwal P, Raich A, Haukaas T (2007) Reliability-based optimal design of electrical transmission towers using multi-objective genetic algorithms. *Comput -Aided Civ Infrastruct Eng* 22(4):282–292
- McDonald M, Mahadevan S (2008) Design optimization with system-level reliability constraints. *J Mech Des* 130(2):021403–1–021403–10
- Mogami K, Nishiwaki S, Izui K, Yoshimura M, Kogiso N (2006) Reliability-based structural optimization of frame structures for multiple failure criteria using topology optimization techniques. *Struct Multidiscip Optim* 32(4):299–311
- Nguyen TH, Song J, Paulino GH (2010) Single-loop system reliability-based design optimization using matrix-based system reliability method: Theory and applications. *J Mech Des* 132(1):011005–1–011005–11
- Nguyen TH, Song J, Paulino GH (2011) Single-loop system reliability-based topology optimization considering statistical dependence between limit-states. *Struct Multidiscip Optim* 44(5):593–611
- Prékopa A (1995) *Stochastic Programming*. Springer, Netherlands
- Rackwitz R (2001) Reliability analysis - a review and some perspectives. *Struct Saf* 23(4):365–395
- Ramos Jr. AS, Paulino GH (2016) Filtering structures out of ground structures – a discrete filtering tool for structural design optimization. *Struct Multidiscip Optim*. Available Online. doi:10.1007/s00158-015-1390-1
- Royset J, Polak E (2004) Reliability-based optimal design using sample average approximations. *Probab Eng Mech* 19(4):331–343
- Royset J, Kiureghian A, Polak E (2001a) Reliability-based optimal design of series structural systems. *J Eng Mech* 127(6):607–614
- Royset J, Kiureghian A, Polak E (2001b) Reliability-based optimal structural design by the decoupling approach. *Reliab Eng Syst Saf* 73(3):213–221
- Royset J, Der Kiureghian A, Polak E (2006) Optimal design with probabilistic objective and constraints. *J Eng Mech* 132(1):107–118

- Rozvany G (2008) Exact analytical solutions for benchmark problems in probabilistic topology optimization. In: EngOpt2008-International Conference on Engineering Optimization, Rio de Janeiro, Brazil
- Rozvany G, Maute K (2011) Analytical and numerical solutions for a reliability-based benchmark example. *Struct Multidiscip Optim* 43(6):745–753
- Rozvany G (2001) Aims, scope, methods, history and unified terminology of computer-aided topology optimization in structural mechanics. *Struct. Multidiscip. Optim.* 21(2):90–108
- Rozvany G, Zhou M, Birker T (1993) Why multi-load topology designs based on orthogonal microstructures are in general non-optimal. *Struct optim* 6(3):200–204
- Schevenels M, Lazarov B, Sigmund O (2011) Robust topology optimization accounting for spatially varying manufacturing errors. *Comput Methods Appl Mech Eng* 200(4952):3613–3627
- Schüeller G, Jensen H (2008) Computational methods in optimization considering uncertainties - an overview. *Comput Methods Appl Mech Eng* 198(1):2–13
- Sokol T (2011) A 99 line code for discretized michell truss optimization written in mathematica. *Struct Multidiscip Optim* 43(2):181–190
- Sutradhar A, Paulino GH, Miller MJ, Nguyen TH (2010) Topological optimization for designing patient-specific large craniofacial segmental bone replacements. *Proc Natl Acad Sci* 107(30):13222–13227
- Svanberg K (1987) The method of moving asymptotes - A new method for structural optimization. *Int J Numer Methods Eng* 24(2):359–373
- Talishi C, Paulino GH, Pereira A, Menezes IFM (2012) PolyTop: A Matlab implementation of a general topology optimization framework using unstructured polygonal finite element meshes. *Struct Multidiscip Optim* 45(3):329–357
- Topping BHV (1992) Mathematical programming techniques for shape optimization of skeletal structures. In: Rozvany G. (ed) *Shape and Layout Optimization of Structural Systems and Optimality Criteria Methods*, Vol. 325 of International Centre for Mechanical Sciences, Springer Vienna, pp 349–375
- Tu J, Choi KK, Park YH (2001) Design Potential Method for Robust System Parameter Design. *AIAA J* 39:667–677
- Uryasev S (1994) Derivatives of probability functions and integrals over sets given by inequalities. *J Comput Appl Math* 56(12):197–223
- Zhang Y, Kiureghian AD (1995) Two improved algorithms for reliability analysis, reliability and optimization of structural systems. In: *Proceedings of the Sixth IFIP WG7. 5 Working Conference on Reliability and Optimization of Structural Systems*, Assisi, Italy, pp 297–304
- Zegard T, Paulino GH (2014) GRAND - Ground structure based topology optimization for arbitrary 2D domains using MATLAB. *Struct Multidiscip Optim* 50(5):861–882
- Zegard T, Paulino GH (2015) GRAND3 - Ground structure based topology optimization for arbitrary 3D domains using MATLAB. *Struct Multidiscip Optim* 52(6):1161–1184. online, 1–24
- Zhao J, Wang C (2014) Robust topology optimization under loading uncertainty based on linear elastic theory and orthogonal diagonalization of symmetric matrices. *Comput Methods Appl Mech Eng* 273(1):204–218